Charged Current Quasielastic Analysis from MINERνA*

Anushree Ghosh†

CBPF - Centro Brasileiro de Pesquisas F sicas,

Rua Dr. Xavier Sigaud 150,

Urca, Rio de Janeiro,

Rio de Janeiro, 22290-180, Brazil

on behalf of the MINERvA Collaboration

(Dated: April 12, 2016)

Abstract

The MINERνA detector situated in Fermilab, is designed to make precision cross-section measurements for scattering processes on various nuclei. In this proceeding, the results of the charged current quasi-elastic (CCQE) analysis using lepton kinematics and with proton kinematics have been presented. Comparison of these with theoretical models suggested that further studies are required to include the additional nuclear effects in the current simulations. The first direct measurement of electron-neutrino quasielastic-like scattering in the few-GeV region of incident neutrino energy has also been presented. All three analyses, discussed here, are carried out on hydrocarbon target.

MINERνA DETECTOR

The MINERνA experiment [1], located at Fermilab, is dedicated to making precise measurement of neutrino-nucleus cross sections in the few-GeV region, which are relevant for neutrino oscillation experiments. The MINERνA detector is situated in the NuMI beamline at Fermilab, along with the MINOS and NOνA experiments. NuMI provides an intense beam of neutrinos and antineutrinos, resulting from the decay of mesons produced by 120 GeV protons impinging on a carbon target. All the results discussed here were generated from data taken between 2010 and 2012 in the low-energy beam configuration, with a peak neutrino energy of about 3 GeV. During this period data from 3.98×10^{20} protons on target were collected in the neutrino mode, and 1.7×10^{20} protons were collected in the antineutrino mode. Since the summer of 2013 MINERνA has been taking data in the NuMI medium energy configuration, with a peak neutrino energy of about 6 GeV.

The central tracking region of the MINERνA detector is constructed from 120 planes of parallel triangular strips of plastic scintillator, arranged almost perpendicular to the beam axis. Each strip contains a wavelength-shifting fiber, which delivers light generated by charged particles to photomultiplier tubes. Targets of water, carbon, iron, and lead are embedded between scintillating strips upstream of the central detector, and a liquid helium target is placed upstream of the main detector. The central detector is surrounded by an electromagnetic and hadronic calorimetery. The magnetized MINOS near detector sits downstream of MINERνA and serves as a muon spectrometer. The results presented in this paper are based on an analysis of interactions in the central, fully-active tracking region.

CCQE INTERACTION

The quasielastic interaction is defined as the process in which a neutrino scatters from a nucleon bound in the nucleus via the exchange of a $W^{\pm}$ boson, thereby emitting a charged lepton and nucleon, with no meson production and minimal energy transfer to spectator nucleons. If the neutrino scatters quasi-elastically from a stationary nucleon, the neutrino energy (E_ν) and momentum transfer Q^2 can be calculated from the polar angle and the momentum of the final state lepton. Alternatively, one can also reconstruct the neutrino energy and the momentum transfer from the final state proton kinematics.

Quasielastic scattering from a bound nucleon is generally modeled as scattering on free nucleons in a relativistic Fermi gas (RFG), with the nucleon axial form factor that measured in neutrino-deuterium quasielastic scattering [2][3]. The RFG model [4] assumes that the initial state nucleons act independently in the mean field of the nucleus and does not include effects due to nucleon-nucleon correlations, as well as interactions of the final state particles within the nucleus, which significantly modify the Fermi gas picture, and thereby affect the neutrino energy reconstruction in oscillation experiments. The hadrons produced in the neutrino-nucleus interactions are subject to final-state interactions (FSI) while propagating through the nucleus. As a result, the inelastic processes with a quasi-elastic-like final state (i.e., no final state mesons) and nucleon-nucleon correlations contribute to the measured quasielastic (QE) cross section having different kinematics and final state hadron content for the same neutrino energy. These processes are particularly important when reconstruction is done using proton kinematics instead of lepton kinematics.

This paper presents the results of a CCQE analysis using both lepton kinematics and proton kinematics on a hydrocarbon target.

CCQE INTERACTION USING LEPTON KINEMATICS

MINERνA has previously measured both neutrino and antineutrino differential cross sections in the fully active central tracking region [5][6]. The neutrino energy and the square of the four momentum transferred to the nucleus, Q^2_{QE} , are estimated from the muon momentum and angle using the quasielastic hypothesis:

$$E_\nu^{QE} = \frac{m_n^2 - (m_p - E_b)^2 - m_\mu^2 + 2(m_p - E_b)E_\mu}{2(m_p - E_b - E_\mu + p_\mu \cos\theta_\mu)} \quad (1)$$

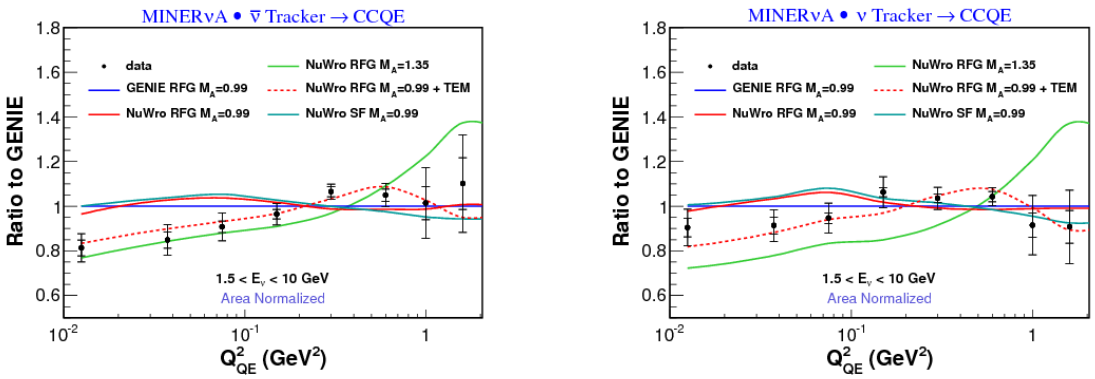

FIG. 1: Left: antineutrino CCQE differential cross-section. Right: neutrino CCQE differential cross section. The events are reconstructed using muon kinematics

$$Q^2_{QE} \;=\; 2E^{QE}_{\nu}(E_\mu - p_\mu \cos\theta_\mu) - m^2_\mu, \tag{2}$$

where E_μ and p_μ are the muon energy and momentum, θ_μ is the muon angle with respect to the beam and m_n, m_p and m_μ are the masses of the neutron, proton and muon, respectively. A selection has been made on the energy and direction of a tracked proton in order to remove the events modified by the FSI or caused by the non-QE processes and hence, increase the QE purity of the sample.

Figure 1 shows the shape-only measured differential cross section distribution as a ratio to the GENIE [7] 2.6.2 Monte Carlo prediction and compared to various theoretical models and M_A values from the NuWro generator [8]. GENIE uses an RFG model, with $M_A = 0.99$ GeV/c^2. Figure 1 also shows the comparison with NuWro generator's RFG models with M_A of 0.99 GeV and 1.35 GeV, as well as with its modeling of nuclear effects using spectral functions (SF) and transverse enhancement (TEM). At high Q^2, our data disfavor $M_A = 1.35 GeV/c^2$ as extracted from fits of the MiniBooNE neutrino quasielastic data. There is very little difference if the RFG nuclear model is replaced with a spectral function (SF) model [9]. For both the neutrino and antineutrino cases, the best agreement is obtained using the lower value of $M_A = 0.99$, along with the empirical transverse enhancement model (TEM), motivated by electron-carbon scattering data [10], which gives an indication of the correlation effects in initial state nucleus.

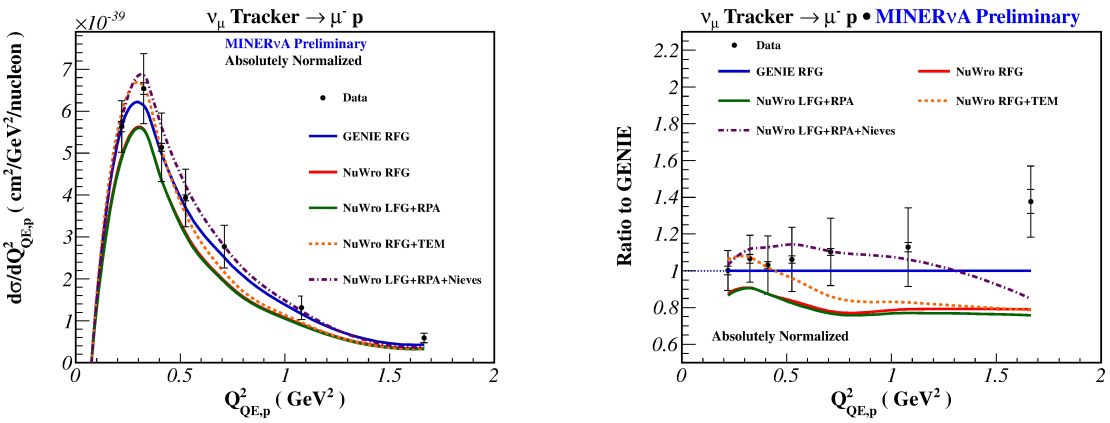

FIG. 2: Neutrino CCQE-like differential cross section. The events are reconstructed using proton kinematics.

CCQE INTERACTION USING PROTON KINEMATICS

The other CCQE analysis [11] presented here uses a sample of CCQE-like events where both the muon and proton are identified. In this analysis, Q^2 is reconstructed using proton kinematics. This eliminates the need for the muon to enter the MINOS detector, which in turn increase angular acceptance. Proton tracks are distinguished from pions by putting a cut on energy deposition rate dE/dx. The events with Michel electrons from the decay of a pion to a muon, which itself decays at rest, are also rejected. The CCQE-like differential cross section as a function of Q^2_p, along with the prediction from GENIE and NuWro using RFG Model, is shown in Fig. 2 (left panel). Various extensions to the NuWro QE RFG prediction are shown, where each prediction represents the sum over all reactions with at least one proton above 110 MeV and no other hadron in the final state. Figure 2 (right panel) shows the comparison of the shape of $\frac{d\sigma}{dQ^2_p}$ between prediction and data. In contrast to the previous analysis, which favored TEM, this analysis shows closest agreement to the RFG with no other modifications. However, there are several important differences between the two analyses. Unlike the one track analysis, in this case, due to the requirement for a trackable proton with a kinetic energy $>$ 110 MeV, the low Q^2 range is restricted. Also, FSI modeling is important here, as the final state proton may affected by FSI interaction as mentioned before.

ELECTRON NEUTRINO SCATTERING

Next, I present the results of the direct measurement of the CCQE-like electron neutrino scattering on nucleons in the central tracker region at an average ν_e energy of 3.6 GeV, which is one of the dominant reaction mechanisms at most energies of interest to oscillation experiments [12]. This analysis focuses on a search for CCQE-like events, i.e., events with either an electron or positron, no other leptons or photons, any number of nucleons, and no other hadrons. Candidate events are selected from the data based on three major criteria. First, a candidate must contain a reconstructed cone object of angle 7.5°; must originate in the fiducial volume, and must be identified as a candidate electromagnetic cascade by a multivariate PID algorithm. Second, electrons and positrons are distinguished from photons by eliminating events in which the energy deposition at the upstream end of the cone is consistent with two particles rather than one. Third, CCQE-like interactions are selected using a classifier called the "extra energy fraction", Ψ. An event's visible energy not associated with the electron candidate or a sphere of radius 30 cm centered around the cone vertex is denoted as "extra energy", defined as:

$$\Psi = \frac{E_{extra}}{E_{electron}} \tag{3}$$

Figure 3 shows the differential ν_e CCQE-like cross sections versus electron energy and angle for both the data and the POT-normalized Monte Carlo samples. The similar distribution in Q^2_{QE} is presented in Fig. 4 (left panel). The simulation procedure appears to underestimate the width of the electron production angle, thereby exhibiting a harder spectrum in Q^2_{QE} . However, these differences are reduced after taking into account the Q^2 dependent correlated errors such as the error in the electromagnetic energy scale.

We also compare the measured differential cross section for ν_e and ν_μ on carbon as a function of Q^2_{QE}, as shown in Fig. 4 (right panel). The data for the differential cross section for ν_e CCQE interactions agree within the errors with that for ν_μ CCQE interactions. Considering the Q^2 dependent correlated errors, the data is consistent with the GENIE prediction within 1σ.

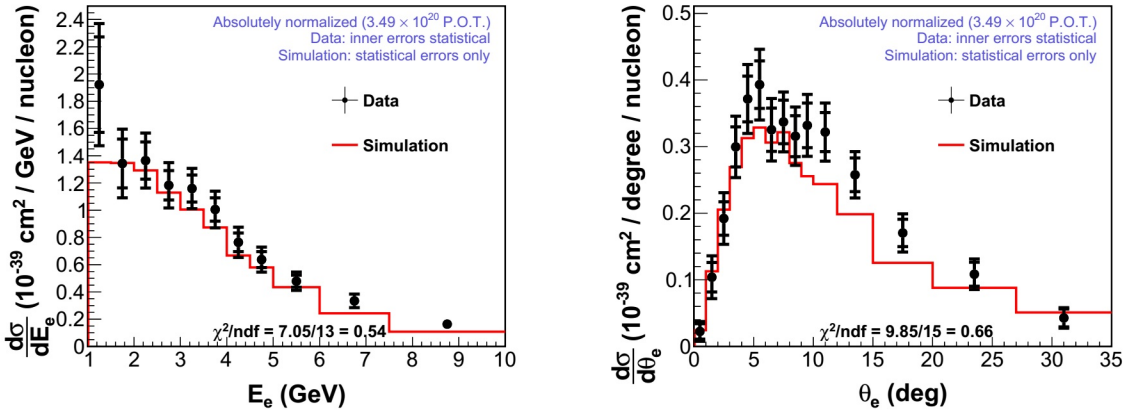

FIG. 3: Left: differential ν_e CCQE-like cross section verses electron energy. Right: differential ν_e CCQE-like cross section verses electron angle.

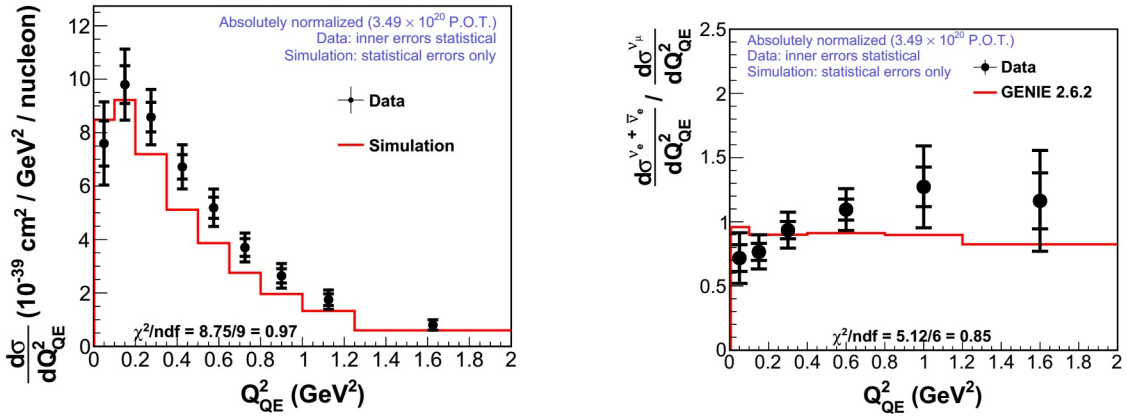

FIG. 4: Left: Differential ν_e CCQE-like cross section verses Q^2_{QE}. Right: ratio of the MINERνA ν_e CCQE differential cross section as a function of Q^2_{QE} to the analogous result from MINERνA for ν_μ.

Acknowledgment

This work was supported by the Fermi National Accelerator Laboratory under US Department of Energy contract No. DE-AC02-07CH11359 which included the MINERνA construction project. Construction support also was granted by the United States National Science Foundation under Award PHY-0619727 and by the University of Rochester. Support for participating scientists was provided by NSF and DOE (USA) by CAPES and CNPq (Brazil), by CoNaCyT (Mexico), byCONICYT (Chile), by CONCYTEC, DGI-PUCP and

IDI/IGI-UNI (Peru), by Latin American Center for Physics (CLAF) and by RAS and the Russian Ministry of Education and Science (Russia). We thank the MINOS Collaboration for use of its near detector data. Finally, we thank the staff of Fermilab for support of the beamline and the detector.

---

* *Presented at NuFact15, 10-15 Aug 2015, Rio de Janeiro, Brazil [C15-08-10.2]*

† `Anushree@cbpf.br`; Speaker

[1] L. Aliaga et al. (MINERvA), Nucl. Instrum. Meth. **A743**, 130 (2014), 1305.5199.

[2] A. Bodek, S. Avvakumov, R. Bradford, and H. Budd, Journal of Physics: Conference Series **110**, 082004 (2008), URL `http://stacks.iop.org/1742-6596/110/i=8/a=082004`.

[3] K. S. Kuzmin, V. V. Lyubushkin, and V. A. Naumov, Eur. Phys. J. **C54**, 517 (2008), 0712.4384.

[4] R. A. Smith and E. J. Moniz, Nucl. Phys. **B43**, 605 (1972), [Erratum: Nucl. Phys.B101,547(1975)].

[5] G. A. Fiorentini et al. (MINERvA), Phys. Rev. Lett. **111**, 022502 (2013), 1305.2243.

[6] L. Fields et al. (MINERvA), Phys. Rev. Lett. **111**, 022501 (2013), 1305.2234.

[7] C. Andreopoulos, C. Barry, S. Dytman, H. Gallagher, T. Golan, R. Hatcher, G. Perdue, and J. Yarba (2015), 1510.05494.

[8] T. Golan, C. Juszczak, and J. T. Sobczyk, Phys. Rev. **C86**, 015505 (2012), 1202.4197.

[9] O. Benhar, A. Fabrocini, S. Fantoni, and I. Sick, Nucl. Phys. **A579**, 493 (1994).

[10] A. Bodek, H. S. Budd, and M. E. Christy, Eur. Phys. J. **C71**, 1726 (2011), 1106.0340.

[11] T. Walton et al. (MINERvA), Phys. Rev. **D91**, 071301 (2015), 1409.4497.

[12] J. Wolcott et al. (MINERvA) (2015), 1509.05729.